Electronic Supplementary Material (ESI) for Physical Chemistry Chemical Physics.

A theoretical study of addition of CH_2OO to hydroxymethyl hydroperoxide and its implications on SO_3 formation in the atmosphere.

Ronald Chow[a] and Daniel K.W. Mok[a,*]

[a] Department of Applied Biology and Chemical Technology, Hong Kong Polytechnic University, Hung Hom, Hong Kong

[*] Corresponding Author, Email: daniel.mok@polyu.edu.hk

Supplementary Materials

Table S1 – The computed and experimental rotational constants of CH_2OO

Method	A (MHz)	B (MHz)	C (MHz)	Reference	MUE
Experimental	77748.9	12465.03	10721.49	38	N/A
MN15-L/MG3S	80307.34	12430.78	10764.54	38	878.58
CCSD(T)-F12a/TZ-F12	78063.79	12530.67	10797.48	38	152.17
B2PLYP-D3/AVTZ	80578.10	12441.38	10777.34	This work	969.57
MN15-L/AVDZ	57079.20	13692.83	11261.81	This work	7479.27
MN15-L/AVTZ	57079.20	13692.83	11261.81	This work	7479.27
M06-2X/AVDZ	57079.20	13692.83	11261.81	This work	7479.27
M06-2X/AVTZ	57079.20	13692.83	11261.81	This work	7479.27

Table S2 – The computed and experimental vibrational frequencies of CH_2OO

The mean unsigned error (MUE) was obtained by averaging the differences between the experimental values and the computed values in the five experimental available vibrational frequencies only.

Experimental	CCSD(T)-F12a/TZ-F12	MN15-L/MG3S*	B2PLYP-D3/AVDZ	B2PLYP-D3/AVTZ	MN15-L/AVDZ	MN15-L/AVTZ	M06-2X/AVDZ	M06-2X/AVTZ
	3250	3191	3329	3309	3290	3262	3311	3291
	3090	3033	3157	3149	3115	3104	3150	3140
1435	1466	1514	1483	1499	1539	1553	1618	1630
1286	1294	1376	1343	1354	1396	1408	1422	1434
1241	1221	1223	1237	1247	1241	1248	1252	1262
908	937	946	975	977	937	958	1010	1023
848	857	915	891	901	917	935	947	929
	630	668	666	673	674	683	697	698
	528	523	538	537	533	531	546	539
Reference	38	38	This work	This work	This work	This work	This work	This work
MUE	19.4	58.4	43.8	52.0	62.4	76.8	106.2	112

*The vibrational frequencies were scaled by a factor of 0.977.

Table S3 Computed (BD(T)/AVTZ//B2PLYP-D3/AVTZ) classical adiabatic ground-state transmission coefficient at the TST ($\kappa^{TST/CAG}$) and the CVT ($\kappa^{CVT/CAG}$) levels and the tunneling correction factors at the ZCT (κ^{ZCT}) and the SCT (κ^{SCT}) levels of channel 2 CH_2OO + $HOCH_2OOH$ $\rightarrow$ $HOCH_2O(O)CH_2OOH$.

T (K)	$\kappa^{TST/CAG}$	$\kappa^{CVT/CAG}$	κ^{ZCT}	κ^{SCT}
200	0.3033	0.9751	1.0000	1.0000
210	0.3210	0.9756	1.0000	1.0000
220	0.3380	0.9762	1.0000	1.0000
230	0.3543	0.9767	1.0000	1.0000
240	0.3700	0.9772	1.0000	1.0000
250	0.3850	0.9777	1.0000	1.0000
260	0.3994	0.9782	1.0000	1.0000
270	0.4132	0.9787	1.0000	1.0000
280	0.4265	0.9792	1.0000	1.0000
290	0.4392	0.9796	1.0000	1.0000
298	0.4490	0.9799	1.0000	1.0000
300	0.4514	0.9800	1.0000	1.0000
310	0.4631	0.9804	1.0000	1.0000
320	0.4744	0.9808	1.0000	1.0000
330	0.4852	0.9812	1.0000	1.0000
340	0.4957	0.9816	1.0000	1.0000
350	0.5057	0.9820	1.0000	1.0000
360	0.5154	0.9823	1.0000	1.0000
370	0.5247	0.9827	1.0000	1.0000
380	0.5337	0.9830	1.0000	1.0000
390	0.5423	0.9833	1.0000	1.0000
400	0.5507	0.9836	1.0000	1.0000

Table S4 Computed (BD(T)/AVTZ//B2PLYP-D3/AVTZ) rate coefficients ($cm^3 molecule^{-1} second^{-1}$) of channel 2 CH_2OO + $HOCH_2OOH \rightarrow HOCH_2O(O)CH_2OOH$ at the TST, the CVT, and the ICVT levels with and without tunneling correction at the SCT level.

T (K)	TST	CVT	ICVT	TST/SCT	CVT/SCT	ICVT/SCT
200	8.41E-07	2.86E-07	2.86E-07	2.55E-07	2.79E-07	2.86E-07
210	3.04E-07	1.09E-07	1.09E-07	9.74E-08	1.07E-07	1.09E-07
220	1.20E-07	4.57E-08	4.57E-08	4.07E-08	4.46E-08	4.57E-08
230	5.18E-08	2.06E-08	2.06E-08	1.84E-08	2.02E-08	2.06E-08
240	2.40E-08	9.98E-09	9.98E-09	8.87E-09	9.75E-09	9.98E-09
250	1.18E-08	5.12E-09	5.12E-09	4.55E-09	5.01E-09	5.12E-09
260	6.15E-09	2.77E-09	2.77E-09	2.46E-09	2.71E-09	2.77E-09
270	3.37E-09	1.57E-09	1.57E-09	1.39E-09	1.54E-09	1.57E-09
280	1.93E-09	9.28E-10	9.28E-10	8.23E-10	9.09E-10	9.28E-10
290	1.15E-09	5.70E-10	5.70E-10	5.05E-10	5.58E-10	5.70E-10
298	7.79E-10	3.95E-10	3.95E-10	3.50E-10	3.87E-10	3.95E-10
300	7.09E-10	3.62E-10	3.62E-10	3.20E-10	3.54E-10	3.62E-10
310	4.52E-10	2.37E-10	2.37E-10	2.10E-10	2.32E-10	2.37E-10
320	2.97E-10	1.59E-10	1.59E-10	1.41E-10	1.56E-10	1.59E-10
330	2.01E-10	1.10E-10	1.10E-10	9.73E-11	1.08E-10	1.10E-10
340	1.39E-10	7.77E-11	7.77E-11	6.87E-11	7.63E-11	7.77E-11
350	9.80E-11	5.60E-11	5.60E-11	4.96E-11	5.50E-11	5.60E-11
360	7.07E-11	4.12E-11	4.12E-11	3.64E-11	4.05E-11	4.12E-11
370	5.20E-11	3.08E-11	3.08E-11	2.73E-11	3.03E-11	3.08E-11
380	3.89E-11	2.35E-11	2.35E-11	2.08E-11	2.31E-11	2.35E-11
390	2.96E-11	1.81E-11	1.81E-11	1.60E-11	1.78E-11	1.81E-11
400	2.28E-11	1.42E-11	1.42E-11	1.26E-11	1.40E-11	1.42E-11

Table S5 Computed k_{outer}, k_{inner}, and $k_{overall}$ (cm^3 $molecule^{-1}s^{-1}$) values of the channel 2 CH_2OO + $HOCH_2OOH$ → $HOCH_2O(O)CH_2OOH$. k_{outer} and k_{inner} were evaluated at the PST and the ICVT levels, respectively and $k_{overall}$ was calculated using equation 1.

T (K)	k_{outer}	k_{inner}	$k_{overall}$
200	2.45E-10	2.86E-07	2.45E-10
210	2.59E-10	1.09E-07	2.58E-10
220	2.74E-10	4.57E-08	2.72E-10
230	2.88E-10	2.06E-08	2.84E-10
240	3.03E-10	9.98E-09	2.94E-10
250	3.17E-10	5.12E-09	2.99E-10
260	3.32E-10	2.77E-09	2.97E-10
270	3.47E-10	1.57E-09	2.84E-10
280	3.62E-10	9.28E-10	2.61E-10
290	3.78E-10	5.70E-10	2.27E-10
298	3.90E-10	3.95E-10	1.96E-10
300	3.93E-10	3.62E-10	1.88E-10
310	4.08E-10	2.37E-10	1.50E-10
320	4.23E-10	1.59E-10	1.16E-10
330	4.39E-10	1.10E-10	8.80E-11
340	4.55E-10	7.77E-11	6.64E-11
350	4.70E-10	5.60E-11	5.01E-11
360	4.86E-10	4.12E-11	3.80E-11
370	5.02E-10	3.08E-11	2.91E-11
380	5.17E-10	2.35E-11	2.24E-11
390	5.33E-10	1.81E-11	1.75E-11
400	5.49E-10	1.42E-11	1.38E-11

Table S6 The computed stabilization rate coefficient ($cm^3molecule^{-1}second^{-1}$) of channel 2 CH_2OO + $HOCH_2OOH$ → $HOCH_2O(O)CH_2OOH$ using the SS-QRRK approach from 0.1 atm to 1.0 atm and from 200 K to 298 K

T (K)	Pressure (atm)	k_{stab} ($cm^3molecule^{-1}second^{-1}$)
200	0.1	6.83E-08
200	0.2	1.10E-07
200	0.3	1.38E-07
200	0.4	1.58E-07
200	0.5	1.73E-07
200	0.6	1.85E-07
200	0.7	1.95E-07
200	0.8	2.03E-07
200	0.9	2.09E-07
200	1.0	2.15E-07
210	0.1	2.44E-08
210	0.2	3.96E-08
210	0.3	5.01E-08
210	0.4	5.78E-08
210	0.5	6.36E-08
210	0.6	6.82E-08
210	0.7	7.19E-08
210	0.8	7.50E-08
210	0.9	7.76E-08
210	1.0	7.99E-08
220	0.1	9.56E-09
220	0.2	1.57E-08
220	0.3	2.00E-08
220	0.4	2.32E-08
220	0.5	2.56E-08
220	0.6	2.76E-08
220	0.7	2.92E-08
220	0.8	3.05E-08
220	0.9	3.16E-08
220	1.0	3.26E-08
230	0.1	4.02E-09
230	0.2	6.66E-09
230	0.3	8.55E-09
230	0.4	9.96E-09
230	0.5	1.11E-08
230	0.6	1.19E-08
230	0.7	1.27E-08
230	0.8	1.33E-08
230	0.9	1.38E-08
230	1.0	1.43E-08
240	0.1	1.81E-09
240	0.2	3.03E-09
240	0.3	3.92E-09
240	0.4	4.59E-09
240	0.5	5.12E-09
240	0.6	5.55E-09
240	0.7	5.90E-09
240	0.8	6.20E-09
240	0.9	6.46E-09
240	1.0	6.68E-09

250	0.1	8.61E-10
250	0.2	1.46E-09
250	0.3	1.89E-09
250	0.4	2.23E-09
250	0.5	2.50E-09
250	0.6	2.72E-09
250	0.7	2.90E-09
250	0.8	3.05E-09
250	0.9	3.19E-09
250	1.0	3.30E-09
260	0.1	4.31E-10
260	0.2	7.35E-10
260	0.3	9.62E-10
260	0.4	1.14E-09
260	0.5	1.28E-09
260	0.6	1.40E-09
260	0.7	1.50E-09
260	0.8	1.58E-09
260	0.9	1.65E-09
260	1.0	1.72E-09
270	0.1	2.25E-10
270	0.2	3.87E-10
270	0.3	5.10E-10
270	0.4	6.07E-10
270	0.5	6.86E-10
270	0.6	7.51E-10
270	0.7	8.07E-10
270	0.8	8.54E-10
270	0.9	8.96E-10
270	1.0	9.32E-10
280	0.1	1.22E-10
280	0.2	2.12E-10
280	0.3	2.81E-10
280	0.4	3.36E-10
280	0.5	3.81E-10
280	0.6	4.19E-10
280	0.7	4.52E-10
280	0.8	4.80E-10
280	0.9	5.04E-10
280	1.0	5.26E-10
290	0.1	6.87E-11
290	0.2	1.20E-10
290	0.3	1.60E-10
290	0.4	1.93E-10
290	0.5	2.20E-10
290	0.6	2.42E-10
290	0.7	2.62E-10
290	0.8	2.79E-10
290	0.9	2.94E-10
290	1.0	3.07E-10
298	0.1	4.43E-11
298	0.2	7.78E-11
298	0.3	1.04E-10
298	0.4	1.26E-10

298	0.5	1.44E-10
298	0.6	1.59E-10
298	0.7	1.73E-10
298	0.8	1.84E-10
298	0.9	1.94E-10
298	1.0	2.04E-10
300	0.1	3.98E-11
300	0.2	7.01E-11
300	0.3	9.42E-11
300	0.4	1.14E-10
300	0.5	1.30E-10
300	0.6	1.44E-10
300	0.7	1.56E-10
300	0.8	1.67E-10
300	0.9	1.76E-10
300	1.0	1.84E-10
310	0.1	2.37E-11
310	0.2	4.21E-11
310	0.3	5.68E-11
310	0.4	6.90E-11
310	0.5	7.92E-11
310	0.6	8.80E-11
310	0.7	9.57E-11
310	0.8	1.02E-10
310	0.9	1.08E-10
310	1.0	1.14E-10
320	0.1	1.44E-11
320	0.2	2.58E-11
320	0.3	3.50E-11
320	0.4	4.27E-11
320	0.5	4.92E-11
320	0.6	5.49E-11
320	0.7	5.99E-11
320	0.8	6.43E-11
320	0.9	6.82E-11
320	1.0	7.17E-11
330	0.1	9.00E-12
330	0.2	1.62E-11
330	0.3	2.21E-11
330	0.4	2.71E-11
330	0.5	3.14E-11
330	0.6	3.51E-11
330	0.7	3.84E-11
330	0.8	4.14E-11
330	0.9	4.40E-11
330	1.0	4.64E-11
340	0.1	5.73E-12
340	0.2	1.04E-11
340	0.3	1.42E-11
340	0.4	1.75E-11
340	0.5	2.04E-11
340	0.6	2.29E-11
340	0.7	2.51E-11
340	0.8	2.71E-11

340	0.9	2.89E-11
340	1.0	3.05E-11
350	0.1	3.70E-12
350	0.2	6.75E-12
350	0.3	9.32E-12
350	0.4	1.15E-11
350	0.5	1.34E-11
350	0.6	1.51E-11
350	0.7	1.67E-11
350	0.8	1.80E-11
350	0.9	1.93E-11
350	1.0	2.04E-11
360	0.1	2.44E-12
360	0.2	4.47E-12
360	0.3	6.20E-12
360	0.4	7.70E-12
360	0.5	9.02E-12
360	0.6	1.02E-11
360	0.7	1.13E-11
360	0.8	1.22E-11
360	0.9	1.31E-11
360	1.0	1.39E-11
370	0.1	1.63E-12
370	0.2	3.00E-12
370	0.3	4.18E-12
370	0.4	5.21E-12
370	0.5	6.13E-12
370	0.6	6.95E-12
370	0.7	7.69E-12
370	0.8	8.37E-12
370	0.9	8.99E-12
370	1.0	9.56E-12
380	0.1	1.10E-12
380	0.2	2.05E-12
380	0.3	2.86E-12
380	0.4	3.59E-12
380	0.5	4.23E-12
380	0.6	4.81E-12
380	0.7	5.34E-12
380	0.8	5.83E-12
380	0.9	6.27E-12
380	1.0	6.69E-12
390	0.1	7.54E-13
390	0.2	1.40E-12
390	0.3	1.98E-12
390	0.4	2.48E-12
390	0.5	2.94E-12
390	0.6	3.36E-12
390	0.7	3.73E-12
390	0.8	4.08E-12
390	0.9	4.41E-12
390	1.0	4.71E-12
400	0.1	5.23E-13
400	0.2	9.80E-13

400	0.3	1.38E-12
400	0.4	1.75E-12
400	0.5	2.07E-12
400	0.6	2.37E-12
400	0.7	2.65E-12
400	0.8	2.90E-12
400	0.9	3.14E-12
400	1.0	3.36E-12

Table S7 Computed (BD(T)/AVTZ//B2PLYP-D3/AVTZ) classical adiabatic ground-state transmission coefficients at the TST and CVT levels ($\kappa^{TST/CAG}$ and $\kappa^{CVT/CAG}$) and computed (BD(T)/AVTZ//B2PLYP-D3/AVTZ) tunneling coefficients at the ZCT and the SCT (κ^{ZCT} and κ^{SCT}) levels of channel 1 CH_2OO + $HOCH_2OOH$ → $HOCH_2OOCH_2OOH$.

T (K)	$\kappa^{TST/CAG}$	$\kappa^{CVT/CAG}$	κ^{ZCT}	κ^{SCT}
200	0.4677	0.9996	1.0000	1.0000
210	0.4849	0.9996	1.0000	1.0000
220	0.5011	0.9995	1.0000	1.0000
230	0.5164	0.9994	1.0000	1.0000
240	0.5308	0.9994	1.0000	1.0000
250	0.5445	0.9993	1.0000	1.0000
260	0.5573	0.9992	1.0000	1.0000
270	0.5695	0.9992	1.0000	1.0000
280	0.5811	0.9991	1.0000	1.0000
290	0.5921	0.9990	1.0000	1.0000
298	0.6005	0.9989	1.0000	1.0000
300	0.6025	0.9989	1.0000	1.0000
310	0.6124	0.9988	1.0000	1.0000
320	0.6219	0.9987	1.0000	1.0000
330	0.6309	0.9986	1.0000	1.0000
340	0.6395	0.9985	1.0000	1.0000
350	0.6477	0.9984	1.0000	1.0000
360	0.6556	0.9982	1.0000	1.0000
370	0.6631	0.9981	1.0000	1.0000
380	0.6703	0.9980	1.0000	1.0000
390	0.6772	0.9978	1.0000	1.0000
400	0.6839	0.9976	1.0000	1.0000

Table S8 Computed (BD(T)/AVTZ//B2PLYP-D3/AVTZ) rate coefficients ($cm^3 molecule^{-1} second^{-1}$) of channel 1 CH_2OO + $HOCH_2OOH \rightarrow HOCH_2OOCH_2OOH$ at the TST, the CVT, and the ICVT levels with and without tunneling correction at the SCT level.

T (K)	TST	CVT	ICVT	TST/SCT	CVT/SCT	ICVT/SCT
200	1.55E-09	8.17E-10	8.17E-10	7.24E-10	8.17E-10	8.17E-10
210	7.71E-10	4.23E-10	4.23E-10	3.74E-10	4.23E-10	4.23E-10
220	4.10E-10	2.33E-10	2.33E-10	2.05E-10	2.33E-10	2.33E-10
230	2.31E-10	1.36E-10	1.36E-10	1.19E-10	1.36E-10	1.36E-10
240	1.37E-10	8.28E-11	8.28E-11	7.26E-11	8.28E-11	8.28E-11
250	8.46E-11	5.27E-11	5.27E-11	4.61E-11	5.27E-11	5.27E-11
260	5.44E-11	3.48E-11	3.48E-11	3.03E-11	3.48E-11	3.48E-11
270	3.63E-11	2.37E-11	2.37E-11	2.07E-11	2.37E-11	2.37E-11
280	2.49E-11	1.67E-11	1.67E-11	1.45E-11	1.67E-11	1.67E-11
290	1.76E-11	1.20E-11	1.20E-11	1.04E-11	1.20E-11	1.20E-11
298	1.36E-11	9.42E-12	9.42E-12	8.15E-12	9.41E-12	9.42E-12
300	1.27E-11	8.88E-12	8.88E-12	7.68E-12	8.87E-12	8.88E-12
310	9.44E-12	6.70E-12	6.70E-12	5.78E-12	6.69E-12	6.70E-12
320	7.13E-12	5.15E-12	5.15E-12	4.44E-12	5.14E-12	5.15E-12
330	5.49E-12	4.03E-12	4.03E-12	3.46E-12	4.02E-12	4.03E-12
340	4.30E-12	3.20E-12	3.20E-12	2.75E-12	3.20E-12	3.20E-12
350	3.42E-12	2.58E-12	2.58E-12	2.21E-12	2.58E-12	2.58E-12
360	2.76E-12	2.11E-12	2.11E-12	1.81E-12	2.11E-12	2.11E-12
370	2.25E-12	1.75E-12	1.75E-12	1.49E-12	1.74E-12	1.75E-12
380	1.86E-12	1.46E-12	1.46E-12	1.25E-12	1.46E-12	1.46E-12
390	1.56E-12	1.24E-12	1.24E-12	1.05E-12	1.23E-12	1.24E-12
400	1.31E-12	1.05E-12	1.05E-12	8.98E-13	1.05E-12	1.05E-12

Table S9 Computed k_{outer}, k_{inner}, and $k_{overall}$ (cm^3 $molecule^{-1}s^{-1}$) values of the channel 1 CH_2OO + $HOCH_2OOH$ → $HOCH_2OOCH_2OOH$. k_{outer} and k_{inner} were evaluated at the PST and the ICVT levels, respectively and $k_{overall}$ was calculated using equation 1.

T (K)	k_{outer}	k_{inner}	$k_{overall}$
200	2.45E-10	8.17E-10	1.88E-10
210	2.59E-10	4.23E-10	1.61E-10
220	2.74E-10	2.33E-10	1.26E-10
230	2.88E-10	1.36E-10	9.22E-11
240	3.03E-10	8.28E-11	6.50E-11
250	3.17E-10	5.27E-11	4.52E-11
260	3.32E-10	3.48E-11	3.15E-11
270	3.47E-10	2.37E-11	2.22E-11
280	3.62E-10	1.67E-11	1.59E-11
290	3.78E-10	1.20E-11	1.17E-11
298	3.9E-10	9.42E-12	9.20E-12
300	3.93E-10	8.88E-12	8.68E-12
310	4.08E-10	6.70E-12	6.59E-12
320	4.23E-10	5.15E-12	5.09E-12
330	4.39E-10	4.03E-12	3.99E-12
340	4.55E-10	3.20E-12	3.18E-12
350	4.7E-10	2.58E-12	2.57E-12
360	4.86E-10	2.11E-12	2.10E-12
370	5.02E-10	1.75E-12	1.74E-12
380	5.17E-10	1.46E-12	1.46E-12
390	5.33E-10	1.24E-12	1.23E-12
400	5.49E-10	1.05E-12	1.05E-12

Table S10 The computed stabilization rate coefficient ($cm^3 molecule^{-1} second^{-1}$) of channel 1 CH_2OO + $HOCH_2OOH$ → $HOCH_2OOCH_2OOH$ using the SS-QRRK approach from 0.1 atm to 1.0 atm and from 200 K to 400 K

T (K)	Pressure (atm)	k_{stab} (cm^3/molecule/second)
200	0.1	8.17E-10
200	0.2	8.17E-10
200	0.3	8.17E-10
200	0.4	8.17E-10
200	0.5	8.17E-10
200	0.6	8.17E-10
200	0.7	8.17E-10
200	0.8	8.17E-10
200	0.9	8.17E-10
200	1.0	8.17E-10
210	0.1	4.23E-10
210	0.2	4.23E-10
210	0.3	4.23E-10
210	0.4	4.23E-10
210	0.5	4.23E-10
210	0.6	4.23E-10
210	0.7	4.23E-10
210	0.8	4.23E-10
210	0.9	4.23E-10
210	1.0	4.23E-10
220	0.1	2.33E-10
220	0.2	2.33E-10
220	0.3	2.33E-10
220	0.4	2.33E-10
220	0.5	2.33E-10
220	0.6	2.33E-10
220	0.7	2.33E-10
220	0.8	2.33E-10
220	0.9	2.33E-10
220	1.0	2.33E-10
230	0.1	1.36E-10
230	0.2	1.36E-10
230	0.3	1.36E-10
230	0.4	1.36E-10
230	0.5	1.36E-10
230	0.6	1.36E-10
230	0.7	1.36E-10
230	0.8	1.36E-10
230	0.9	1.36E-10
230	1.0	1.36E-10
240	0.1	8.28E-11
240	0.2	8.28E-11
240	0.3	8.28E-11
240	0.4	8.28E-11
240	0.5	8.28E-11
240	0.6	8.28E-11
240	0.7	8.28E-11
240	0.8	8.28E-11
240	0.9	8.28E-11
240	1.0	8.28E-11

250	0.1	5.27E-11
250	0.2	5.27E-11
250	0.3	5.27E-11
250	0.4	5.27E-11
250	0.5	5.27E-11
250	0.6	5.27E-11
250	0.7	5.27E-11
250	0.8	5.27E-11
250	0.9	5.27E-11
250	1.0	5.27E-11
260	0.1	3.48E-11
260	0.2	3.48E-11
260	0.3	3.48E-11
260	0.4	3.48E-11
260	0.5	3.48E-11
260	0.6	3.48E-11
260	0.7	3.48E-11
260	0.8	3.48E-11
260	0.9	3.48E-11
260	1.0	3.48E-11
270	0.1	2.37E-11
270	0.2	2.37E-11
270	0.3	2.37E-11
270	0.4	2.37E-11
270	0.5	2.37E-11
270	0.6	2.37E-11
270	0.7	2.37E-11
270	0.8	2.37E-11
270	0.9	2.37E-11
270	1.0	2.37E-11
280	0.1	1.67E-11
280	0.2	1.67E-11
280	0.3	1.67E-11
280	0.4	1.67E-11
280	0.5	1.67E-11
280	0.6	1.67E-11
280	0.7	1.67E-11
280	0.8	1.67E-11
280	0.9	1.67E-11
280	1.0	1.67E-11
290	0.1	1.20E-11
290	0.2	1.20E-11
290	0.3	1.20E-11
290	0.4	1.20E-11
290	0.5	1.20E-11
290	0.6	1.20E-11
290	0.7	1.20E-11
290	0.8	1.20E-11
290	0.9	1.20E-11
290	1.0	1.20E-11
298	0.1	9.42E-12
298	0.2	9.42E-12
298	0.3	9.42E-12
298	0.4	9.42E-12

298	0.5	9.42E-12
298	0.6	9.42E-12
298	0.7	9.42E-12
298	0.8	9.42E-12
298	0.9	9.42E-12
298	1.0	9.42E-12
300	0.1	8.88E-12
300	0.2	8.88E-12
300	0.3	8.88E-12
300	0.4	8.88E-12
300	0.5	8.88E-12
300	0.6	8.88E-12
300	0.7	8.88E-12
300	0.8	8.88E-12
300	0.9	8.88E-12
300	1.0	8.88E-12
310	0.1	6.70E-12
310	0.2	6.70E-12
310	0.3	6.70E-12
310	0.4	6.70E-12
310	0.5	6.70E-12
310	0.6	6.70E-12
310	0.7	6.70E-12
310	0.8	6.70E-12
310	0.9	6.70E-12
310	1.0	6.70E-12
320	0.1	5.15E-12
320	0.2	5.15E-12
320	0.3	5.15E-12
320	0.4	5.15E-12
320	0.5	5.15E-12
320	0.6	5.15E-12
320	0.7	5.15E-12
320	0.8	5.15E-12
320	0.9	5.15E-12
320	1.0	5.15E-12
330	0.1	4.03E-12
330	0.2	4.03E-12
330	0.3	4.03E-12
330	0.4	4.03E-12
330	0.5	4.03E-12
330	0.6	4.03E-12
330	0.7	4.03E-12
330	0.8	4.03E-12
330	0.9	4.03E-12
330	1.0	4.03E-12
340	0.1	3.20E-12
340	0.2	3.20E-12
340	0.3	3.20E-12
340	0.4	3.20E-12
340	0.5	3.20E-12
340	0.6	3.20E-12
340	0.7	3.20E-12
340	0.8	3.20E-12

340	0.9	3.20E-12
340	1.0	3.20E-12
350	0.1	2.58E-12
350	0.2	2.58E-12
350	0.3	2.58E-12
350	0.4	2.58E-12
350	0.5	2.58E-12
350	0.6	2.58E-12
350	0.7	2.58E-12
350	0.8	2.58E-12
350	0.9	2.58E-12
350	1.0	2.58E-12
360	0.1	2.11E-12
360	0.2	2.11E-12
360	0.3	2.11E-12
360	0.4	2.11E-12
360	0.5	2.11E-12
360	0.6	2.11E-12
360	0.7	2.11E-12
360	0.8	2.11E-12
360	0.9	2.11E-12
360	1.0	2.11E-12
370	0.1	1.75E-12
370	0.2	1.75E-12
370	0.3	1.75E-12
370	0.4	1.75E-12
370	0.5	1.75E-12
370	0.6	1.75E-12
370	0.7	1.75E-12
370	0.8	1.75E-12
370	0.9	1.75E-12
370	1.0	1.75E-12
380	0.1	1.46E-12
380	0.2	1.46E-12
380	0.3	1.46E-12
380	0.4	1.46E-12
380	0.5	1.46E-12
380	0.6	1.46E-12
380	0.7	1.46E-12
380	0.8	1.46E-12
380	0.9	1.46E-12
380	1.0	1.46E-12
390	0.1	1.24E-12
390	0.2	1.24E-12
390	0.3	1.24E-12
390	0.4	1.24E-12
390	0.5	1.24E-12
390	0.6	1.24E-12
390	0.7	1.24E-12
390	0.8	1.24E-12
390	0.9	1.24E-12
390	1.0	1.24E-12
400	0.1	1.05E-12
400	0.2	1.05E-12

400	0.3	1.05E-12
400	0.4	1.05E-12
400	0.5	1.05E-12
400	0.6	1.05E-12
400	0.7	1.05E-12
400	0.8	1.05E-12
400	0.9	1.05E-12
400	1.0	1.05E-12

Table S11 Computed (BD(T)/AVTZ//B2PLYP-D3/AVTZ) $k_{overall}$ ($cm^3 molecule^{-1} second^{-1}$) of both channels 1 CH_2OO + $HOCH_2OOH \rightarrow HOCH_2OOCH_2OOH$ (k_1) and 2 CH_2OO + $HOCH_2OOH \rightarrow HOCH_2O(O)CH_2OOH$ (k_2) and their ratio, k_2/k_1.

T (K)	$k_{overall}$ (channel 1), k_1	$k_{overall}$ (channel 2), k_2	k_2/k_1
200	1.88E-10	2.45E-10	1.30
210	1.61E-10	2.58E-10	1.60
220	1.26E-10	2.72E-10	2.16
230	9.22E-11	2.84E-10	3.08
240	6.50E-11	2.94E-10	4.52
250	4.52E-11	2.99E-10	6.62
260	3.15E-11	2.97E-10	9.43
270	2.22E-11	2.84E-10	12.79
280	1.59E-11	2.61E-10	16.42
290	1.17E-11	2.27E-10	19.40
298	9.20E-12	1.96E-10	21.30
300	8.68E-12	1.88E-10	21.66
310	6.59E-12	1.50E-10	22.76
320	5.09E-12	1.16E-10	22.79
330	3.99E-12	8.80E-11	22.06
340	3.18E-12	6.64E-11	20.88
350	2.57E-12	5.01E-11	19.49
360	2.10E-12	3.80E-11	18.10
370	1.74E-12	2.91E-11	16.72
380	1.46E-12	2.24E-11	15.34
390	1.23E-12	1.75E-11	14.23
400	1.05E-12	1.38E-11	13.14

Table S12 Computed (BD(T)/AVTZ//M06-2X/AVDZ) rate coefficients ($cm^3 molecule^{-1} second^{-1}$) of the $HOCH_2O(O)CH_2OOH + SO_2 \rightarrow HOCH_2OCH_2OOH + SO_3$ reaction at the TST level.

T (K)	TST ($cm^3 molecule^{-1} second^{-1}$)
200.00	1.87E-07
210.00	7.78E-08
220.00	3.52E-08
230.00	1.72E-08
240.00	8.92E-09
250.00	4.91E-09
260.00	2.84E-09
270.00	1.72E-09
280.00	1.08E-09
290.00	7.08E-10
298.00	5.15E-10
300.00	4.77E-10
310.00	3.31E-10
320.00	2.35E-10
330.00	1.71E-10
340.00	1.28E-10
350.00	9.69E-11
360.00	7.49E-11
370.00	5.88E-11
380.00	4.69E-11
390.00	3.79E-11
400.00	3.10E-11

Table S13 Computed k_{outer}, k_{inner}, and $k_{overall}$ (cm^3 $molecule^{-1}s^{-1}$) values of the channel 1 OH + $HOCH_2OOH$ → HOCHOOH + H_2O. k_{outer} and k_{inner} were evaluated at the PST and the ICVT levels, respectively and $k_{overall}$ was calculated using equation 1.

T (K)	k_{outer}	k_{inner}	$k_{overall}$
200	2.42E-09	1.41E-12	1.41E-12
210	2.56E-09	1.26E-12	1.26E-12
220	2.71E-09	1.14E-12	1.14E-12
230	2.85E-09	1.04E-12	1.04E-12
240	3.00E-09	9.54E-13	9.54E-13
250	3.14E-09	8.86E-13	8.86E-13
260	3.29E-09	8.29E-13	8.29E-13
270	3.44E-09	7.81E-13	7.81E-13
280	3.59E-09	7.40E-13	7.40E-13
290	3.74E-09	7.05E-13	7.05E-13
298	3.81E-09	6.89E-13	6.89E-13
300	3.86E-09	6.80E-13	6.80E-13
310	3.89E-09	6.75E-13	6.75E-13
320	4.04E-09	6.48E-13	6.48E-13
330	4.19E-09	6.24E-13	6.23E-13
340	4.35E-09	6.02E-13	6.02E-13
350	4.50E-09	5.84E-13	5.84E-13
360	4.65E-09	5.68E-13	5.68E-13
370	4.81E-09	5.54E-13	5.54E-13
380	4.97E-09	5.41E-13	5.41E-13
390	5.12E-09	5.31E-13	5.31E-13
400	5.28E-09	5.21E-13	5.21E-13

Figure S1 Optimized geometries of $OHCH_2OOH$ at the M06-2X/AVTZ, MN15-L/AVTZ, and B2PLYP-D3/AVTZ levels using ultrafine grids.

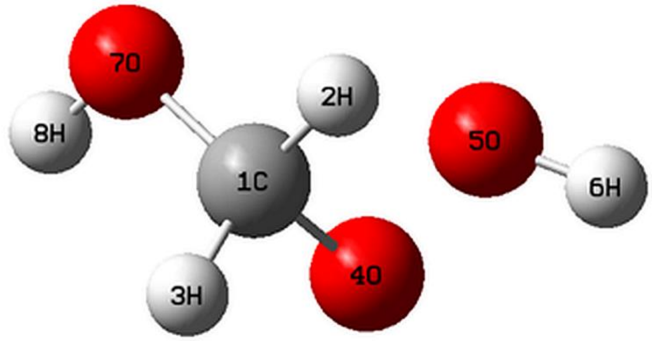

Geometrical parameters	M06-2X/AVTZ	MN15-L/AVTZ	B2PLYP-D3/AVTZ
1C-2H	1.08898 Å	1.10429 Å	1.08719 Å
1C-3H	1.09381 Å	1.11085 Å	1.09345 Å
1C-4O	1.40224 Å	1.40402 Å	1.40834 Å
1C-7O	1.38717 Å	1.39073 Å	1.39413 Å
7O-8H	0.96170 Å	0.96584 Å	0.96275 Å
4O-5O	1.42482 Å	1.44879 Å	1.45977 Å
5O-6H	0.96446 Å	0.96971 Å	0.96638 Å
∠8H-7O-1C	108.92527°	108.02719°	108.62882°
∠7O-1C-4O	113.31017°	113.66508°	113.91534°
∠3H-1C-2H	111.15275°	111.03293°	111.37170°
∠1C-4O-5O	107.63745°	106.76604°	107.11094°
∠4O-5O-6H	100.88849°	99.73793°	99.29819°

Optimized geometries of CH_2OO at the M06-2X/AVTZ, MN15-L/AVTZ, and B2PLYP-D3/AVTZ levels using ultrafine grids

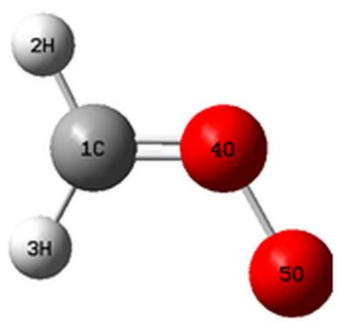

Geometrical parameters	M06-2X/AVTZ	MN15-L/AVTZ	B2PLYP-D3/AVTZ
1C-2H	1.08121 Å	1.09236 Å	1.08101 Å
1C-3H	1.08409 Å	1.09562 Å	1.07775 Å
1C-4O	1.23895 Å	1.25934 Å	1.26669 Å
4O-5O	1.34329 Å	1.34545 Å	1.33788 Å
∠2H-1C-3H	125.43461°	125.64690°	126.18340°
∠2H-1C-4O	115.84460°	115.02397°	114.85897°
∠3H-1C-4O	118.72079°	119.32910°	118.95762°
∠1C-4O-5O	118.65987°	119.01192°	119.15792°
∠3H-1C-4O-5O	0.02154°	0.04036°	-0.00215°

Figure S2 Optimized geometries of the reactant complex, the transition state, and the product in channel 1 CH_2OO + $HOCH_2OOH \rightarrow HOCH_2OOCH_2OOH$ using ultrafine grids

Reactant Complex (RC1) of channel 1 $CH_2OO + HOCH_2OOH \rightarrow HOCH_2OOCH_2OOH$

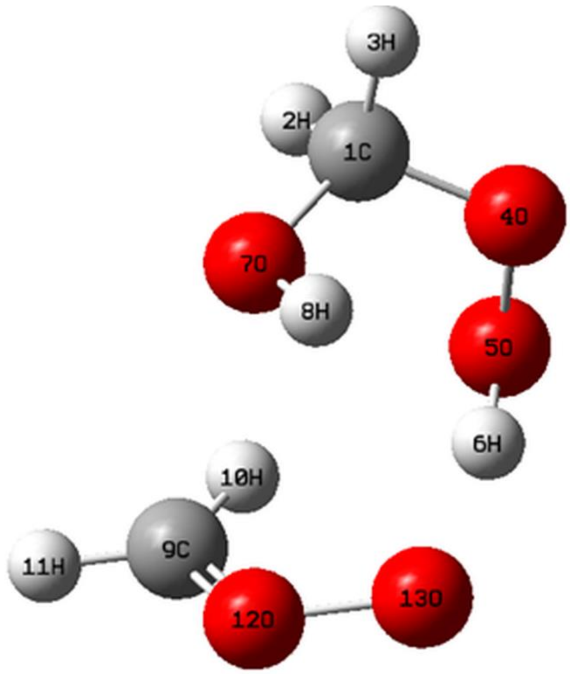

Geometrical parameters	M06-2X/AVTZ	B2PLYP-D3/AVTZ
1C-2H	1.09026 Å	1.08757 Å
1C-3H	1.09228 Å	1.09147 Å
1C-4O	1.38871 Å	1.39337 Å
4O-5O	1.42182 Å	1.45342 Å
5O-6H	0.99012 Å	0.99212 Å
1C-7O	1.40523 Å	1.41526 Å
7O-8H	0.96569 Å	0.96432 Å
8H-10H	2.99905 Å	3.23009 Å
9C-10H	1.08444 Å	1.08075 Å
9C-11H	1.08310 Å	1.07959 Å
9C-12O	1.23463 Å	1.25341 Å
12O-13O	1.37378 Å	1.37515 Å
13O-6H	1.72206 Å	1.72401 Å
∠2H-1C-3H	111.18370°	111.43040°
∠7O-1C-4O	112.60357°	113.58192°
∠1C-4O-5O	108.13099°	107.59711°
∠4O-5O-6H	101.56723°	101.45138°
∠1C-7O-8H	107.73262°	107.74596°
∠8H-10H-9C	74.89438°	71.42929°
∠10H-9C-11H	124.53458°	125.06601°
∠10H-9C-12O	120.33639°	120.25897°
∠9C-12O-13O	118.14591°	118.45602°
∠12O-13O-6H	111.93533°	110.31731°

The optimized geometry of the reactant complex of channel 1 CH_2OO + $HOCH_2OOH$ → $HOCH_2OOCH_2OOH$ obtained at the MN15-L/AVTZ using ultrafine grids

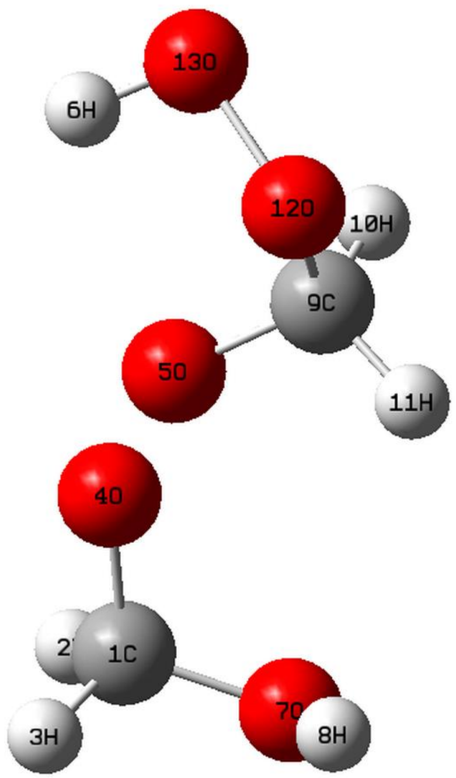

Geometrical parameters	MN15-L/AVTZ
1C-2H	1.10259 Å
1C-3H	1.10862 Å
1C-7O	1.39628 Å
7O-8H	0.96556 Å
1C-4O	1.40548 Å
4O-5O	1.45502 Å
5O-9C	1.40232 Å
9C-12O	1.39318 Å
9C-11H	1.10456 Å
9C-10H	1.10652 Å
12O-13O	1.44086 Å
13O-6H	0.97229 Å
6H-5O	2.52723 Å
∠2H-1C-3H	111.05363°
∠3H-1C-7O	112.98781°
∠1C-7O-8H	108.27558°
∠1C-4O-5O	106.03610°
∠4O-5O-9C	107.49178°
∠5O-9C-10H	103.19933°
∠5O-9C-12O	113.23111°
∠12O-13O-6H	101.04044°

Transition state (TS1) of channel 1 $CH_2OO + HOCH_2OOH \rightarrow HOCH_2OOCH_2OOH$

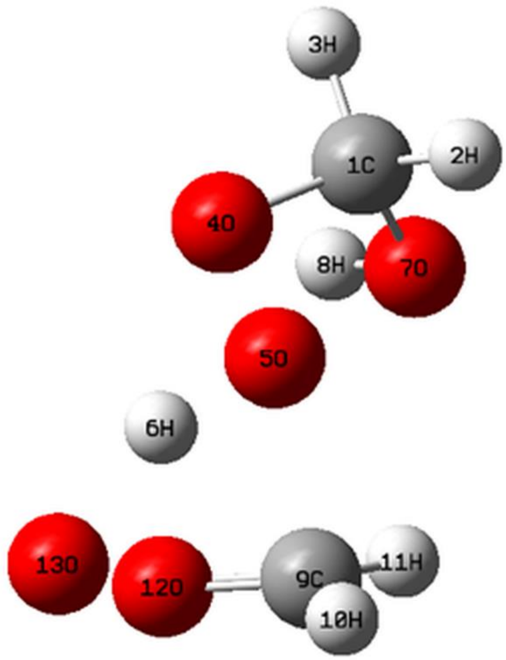

Geometrical parameters	M06-2X/AVTZ	MN15-L/AVTZ	B2PLYP-D3/AVTZ
1C-2H	1.08856 Å	1.10303 Å	1.08679 Å
1C-3H	1.09140 Å	1.10760 Å	1.09086 Å
1C-4O	1.39381 Å	1.40008 Å	1.40198 Å
4O-5O	1.42015 Å	1.43854 Å	1.45238 Å
5O-6H	1.08656 Å	1.08906 Å	1.08508 Å
1C-7O	1.40011 Å	1.40055 Å	1.40640 Å
7O-8H	0.96232 Å	0.96655 Å	0.96295 Å
13O-6H	1.41723 Å	1.43169 Å	1.43800 Å
12O-13O	1.41880 Å	1.43564 Å	1.43962 Å
9C-12O	1.25470 Å	1.27343 Å	1.26683 Å
9C-11H	1.08330 Å	1.09584 Å	1.08140 Å
9C-10H	1.08347 Å	1.09694 Å	1.08080 Å
∠2H-1C-3H	111.22878°	111.20829°	111.43342°
∠7O-1C-4O	112.96398°	113.29886°	113.61050°
∠1C-4O-5O	107.78529°	107.62945°	107.04351°
∠4O-5O-6H	100.29584°	97.89735°	100.20639°
∠1C-7O-8H	108.41907°	107.61467°	108.23451°
∠5O-6H-13O	151.39903°	151.40803°	151.98182°
∠9C-12O-13O	108.42603°	106.75646°	107.81870°
∠10H-9C-12O	119.43107°	119.18681°	119.58643°
∠10H-9C-11H	122.60822°	122.34959°	122.69189°
∠12O-13O-6H	88.09862°	87.50861°	87.75231°

Product ($HOCH_2OOCH_2OOH$) of channel 1 $CH_2OO + HOCH_2OOH \rightarrow HOCH_2OOCH_2OOH$

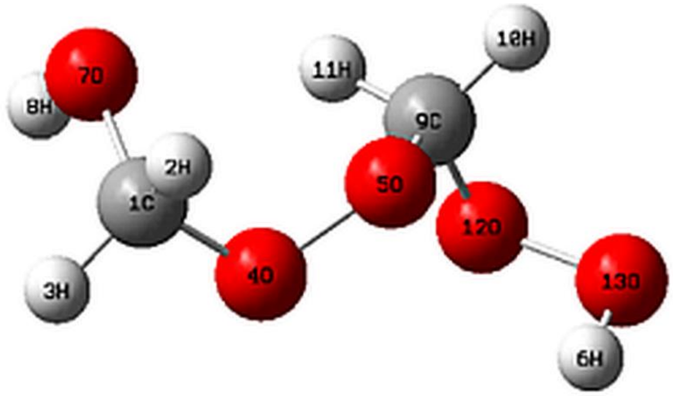

Geometrical parameters	M06-2X/AVTZ	MN15-L/AVTZ	B2PLYP-D3/AVTZ
1C-2H	1.08777 Å	1.10260 Å	1.08621 Å
1C-3H	1.09209 Å	1.10864 Å	1.09177 Å
1C-4O	1.40314 Å	1.40554 Å	1.40940 Å
4O-5O	1.42569 Å	1.45517 Å	1.46202 Å
5O-9C	1.40056 Å	1.40247 Å	1.40522 Å
1C-7O	1.39267 Å	1.39615 Å	1.39983 Å
7O-8H	0.96137 Å	0.96557 Å	0.96235 Å
13O-6H	0.96676 Å	0.97231 Å	0.96812 Å
12O-13O	1.41882 Å	1.44086 Å	1.45104 Å
9C-12O	1.39040 Å	1.39313 Å	1.39702 Å
9C-11H	1.08845 Å	1.10449 Å	1.08772 Å
9C-10H	1.09068 Å	1.10653 Å	1.09008 Å
∠2H-1C-3H	111.18982°	111.04580°	111.33708°
∠7O-1C-4O	113.17495°	113.61121°	113.80971°
∠1C-4O-5O	107.04955°	106.01290°	106.49665°
∠4O-5O-9C	108.50424°	107.49319°	108.03081°
∠1C-7O-8H	109.17519°	108.27289°	108.78700°
∠5O-9C-12O	112.76369°	113.21562°	113.79209°
∠9C-12O-13O	107.68131°	107.00372°	107.36433°
∠10H-9C-12O	111.05922°	111.64601°	111.14579°
∠10H-9C-11H	112.78412°	112.77663°	112.79257°
∠12O-13O-6H	102.06917°	101.03681°	100.88150°

Figure S3 Optimized geometries of the reactant complex, the transition state, and the product in channel 2 CH_2OO + $HOCH_2OOH \rightarrow HOCH_2O(O)CH_2OOH$

Reactant complex (RC2) of channel 2 CH_2OO + $HOCH_2OOH \rightarrow HOCH_2O(O)CH_2OOH$

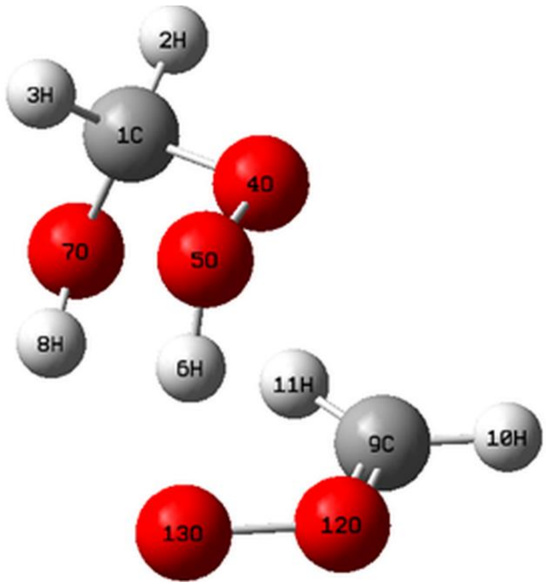

Geometrical parameters	M06-2X/AVTZ	MN15-L/AVTZ	B2PLYP-D3/AVTZ
1C-2H	1.08872 Å	1.10244 Å	1.08766 Å
1C-3H	1.09069 Å	1.10839 Å	1.08950 Å
1C-4O	1.40455 Å	1.39826 Å	1.40299 Å
4O-5O	1.42446 Å	1.45603 Å	1.45883 Å
5O-6H	0.98412 Å	0.98676 Å	0.98854 Å
1C-7O	1.39745 Å	1.40284 Å	1.40825 Å
7O-8H	0.96796 Å	0.96577 Å	0.96408 Å
13O-6H	1.76301 Å	1.85635 Å	1.73574 Å
12O-13O	1.38327 Å	1.36943 Å	1.37617 Å
9C-12O	1.23305 Å	1.25314 Å	1.25265 Å
9C-11H	1.08623 Å	1.09471 Å	1.08441 Å
9C-10H	1.08384 Å	1.09389 Å	1.08071 Å
∠2H-1C-3H	111.29990°	111.18628°	111.53326°
∠7O-1C-4O	112.51691°	113.12941°	113.00949°
∠1C-4O-5O	108.35578°	104.18732°	106.14045°
∠4O-5O-6H	102.42276°	98.34969°	100.55402°
∠1C-7O-8H	109.02005°	106.61104°	107.83277°
∠5O-6H-13O	160.79543°	160.27395°	171.71232°
∠9C-12O-13O	117.13259°	118.12034°	117.55171°
∠10H-9C-12O	115.05544°	115.16896°	114.35274°
∠10H-9C-11H	125.30559°	124.72366°	125.90750°
∠12O-13O-6H	92.34066°	105.10903°	105.74464°

Transition state (TS2) of channel 2 $CH_2OO + HOCH_2OOH \rightarrow HOCH_2O(O)CH_2OOH$

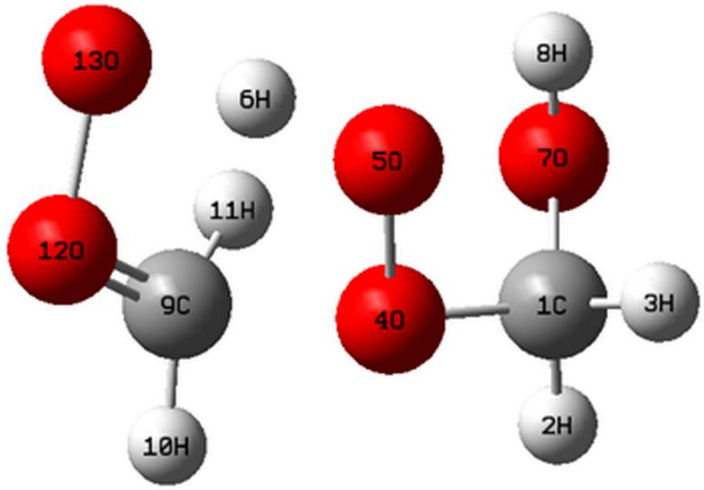

Geometrical parameters	M06-2X/AVTZ	MN15-L/AVTZ	B2PLYP-D3/AVTZ
1C-2H	1.08822 Å	1.10278 Å	1.08746 Å
1C-3H	1.09080 Å	1.10585 Å	1.08857 Å
1C-4O	1.42098 Å	1.43562 Å	1.44126 Å
4O-5O	1.43742 Å	1.45482 Å	1.47142 Å
5O-6H	1.09444 Å	1.13939 Å	1.12968 Å
1C-7O	1.38125 Å	1.38046 Å	1.38174 Å
7O-8H	0.96446 Å	0.96908 Å	0.96599 Å
13O-6H	1.37577 Å	1.31705 Å	1.32299 Å
12O-13O	1.43257 Å	1.45143 Å	1.46911 Å
9C-12O	1.25584 Å	1.27634 Å	1.27161 Å
9C-11H	1.08380 Å	1.09698 Å	1.08129 Å
9C-10H	1.08488 Å	1.09894 Å	1.08339 Å
∠2H-1C-3H	111.57670°	111.88790°	111.83632°
∠7O-1C-4O	111.83654°	112.21721°	112.42338°
∠1C-4O-5O	105.27887°	104.53620°	105.11854°
∠4O-5O-6H	100.86459°	98.26857°	101.15596°
∠1C-7O-8H	107.46759°	106.26539°	107.08840°
∠5O-6H-13O	165.88368°	166.41537°	166.92207°
∠9C-12O-13O	110.88913°	109.57632°	108.25846°
∠10H-9C-12O	115.18130°	114.36567°	114.22620°
∠10H-9C-11H	121.72591°	121.18065°	121.58125°
∠12O-13O-6H	94.50282°	95.71147°	108.25846°

Product ($HOCH_2O(O)CH_2OOH$) of channel 2 $CH_2OO + HOCH_2OOH \rightarrow HOCH_2O(O)CH_2OOH$

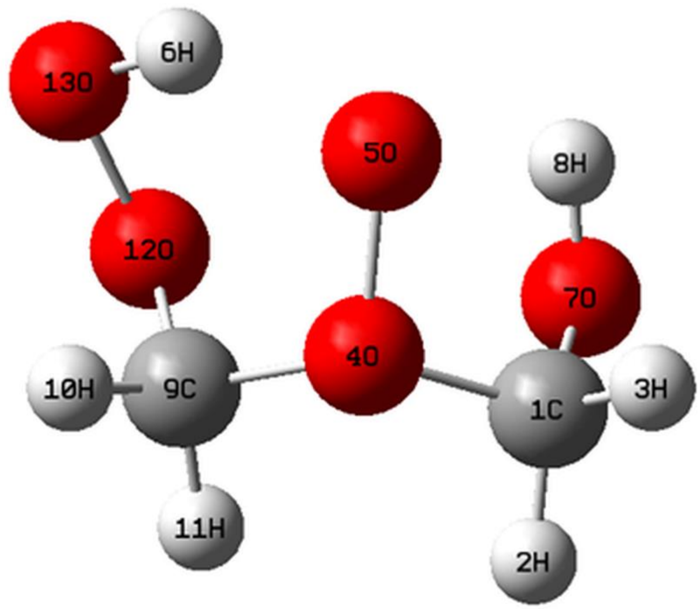

Geometrical parameters	M06-2X/AVTZ	MN15-L/AVTZ	B2PLYP-D3/AVTZ
1C-2H	1.08814 Å	1.10324 Å	1.08662 Å
1C-3H	1.08834 Å	1.10320 Å	1.08716 Å
1C-4O	1.46641 Å	1.48047 Å	1.49032 Å
4O-5O	1.44819 Å	1.46598 Å	1.47477 Å
4O-9C	1.48063 Å	1.50097 Å	1.50925 Å
1C-7O	1.35743 Å	1.35940 Å	1.35774 Å
7O-8H	0.96935 Å	0.97458 Å	0.97177 Å
13O-6H	0.98923 Å	0.98953 Å	0.99795 Å
12O-13O	1.42539 Å	1.44532 Å	1.45865 Å
9C-12O	1.35274 Å	1.35405 Å	1.35076 Å
9C-11H	1.08838 Å	1.10313 Å	1.08723 Å
9C-10H	1.08694 Å	1.10011 Å	1.08510 Å
∠2H-1C-3H	112.60847°	112.86312°	112.89764°
∠7O-1C-4O	111.27739°	111.26195°	111.68195°
∠1C-4O-5O	106.18803°	104.86309°	104.98274°
∠5O-4O-9C	110.06278°	109.30540°	109.47718°
∠1C-7O-8H	106.46557°	105.10036°	105.50109°
∠5O-6H-13O	143.77178°	141.83517°	148.62056°
∠9C-12O-13O	108.52306°	108.03716°	107.71159°
∠10H-9C-12O	112.57170°	112.93128°	113.32317°
∠10H-9C-11H	114.25621°	114.65546°	114.66919°
∠12O-13O-6H	98.58789°	97.68573°	97.13937°

Figure S4 Optimized geometries of the reactant complex, the transition state, and the product in channel 3 CH_2OO + $HOCH_2OOH \rightarrow HOOCH_2OCH_2OOH$

Reactant complex (RC3) of channel 3 $CH_2OO + HOCH_2OOH \rightarrow HOOCH_2OCH_2OOH$

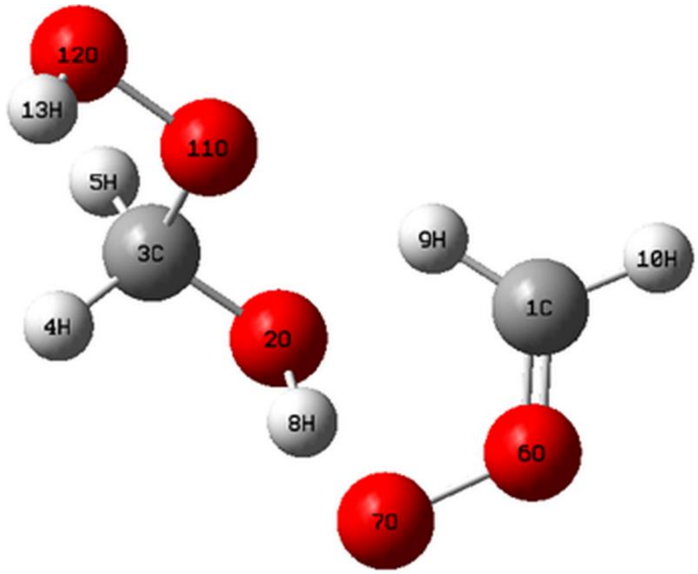

Geometrical parameters	M06-2X/AVTZ	MN15-L/AVTZ	B2PLYP-D3/AVTZ
1C-9H	1.08664 Å	1.09517 Å	1.08081 Å
1C-10H	1.08352 Å	1.09370 Å	1.07971 Å
1C-6O	1.23536 Å	1.25595 Å	1.25276 Å
6O-7O	1.37295 Å	1.36397 Å	1.37848 Å
7O-8H	1.70086 Å	1.98740 Å	1.72298 Å
8H-2O	0.98736 Å	0.97609 Å	0.98845 Å
2O-3C	1.36771 Å	1.38230 Å	1.37023 Å
3C-4H	1.09548 Å	1.11471 Å	1.09364 Å
3C-5H	1.08932 Å	1.10613 Å	1.08740 Å
3C-11O	1.43978 Å	1.42510 Å	1.45535 Å
11O-12O	1.41582 Å	1.43989 Å	1.44872 Å
12O-13H	0.96559 Å	0.97055 Å	0.96772 Å
∠9H-1C-10H	125.05825°	125.26341°	124.80524°
∠1C-6O-7O	117.45586°	118.12924°	117.96022°
∠6O-7O-8H	96.90994°	97.57958°	105.52123°
∠7O-8H-2O	161.20420°	142.90438°	165.05571°
∠4H-3C-5H	110.62336°	110.33902°	111.16444°
∠2O-3C-11O	106.98797°	106.35601°	106.31974°
∠11O-12O-13H	102.47293°	100.80078°	101.42503°

Transition state (TS3) of channel 3 $CH_2OO + HOCH_2OOH \rightarrow HOOCH_2OCH_2OOH$

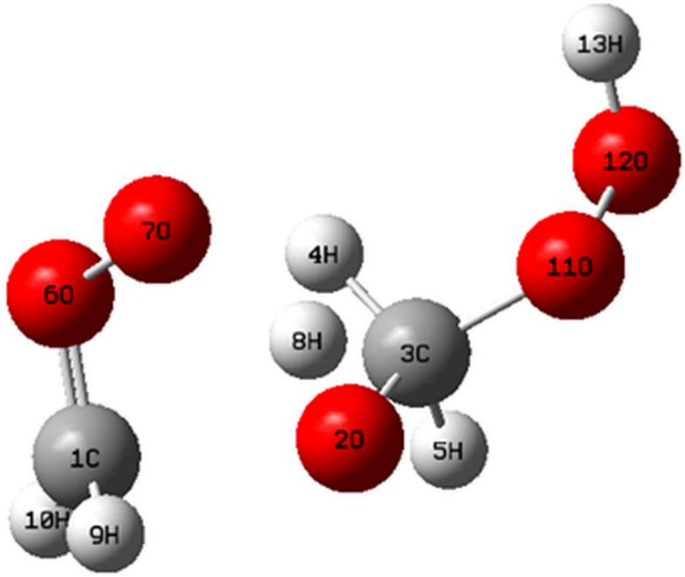

Geometrical parameters	M06-2X/AVTZ	MN15-L/AVTZ	B2PLYP-D3/AVTZ
1C-9H	1.08256 Å	1.09612 Å	1.08008 Å
1C-10H	1.08575 Å	1.09964 Å	1.08399 Å
1C-6O	1.25782 Å	1.27766 Å	1.27196 Å
6O-7O	1.42506 Å	1.44543 Å	1.45095 Å
7O-8H	1.50506 Å	1.48525 Å	1.46662 Å
8H-2O	1.05637 Å	1.07063 Å	1.07636 Å
2O-3C	1.38957 Å	1.39959 Å	1.39860 Å
3C-4H	1.09600 Å	1.11154 Å	1.09325 Å
3C-5H	1.09104 Å	1.10687 Å	1.09001 Å
3C-11O	1.41574 Å	1.41545 Å	1.42308 Å
11O-12O	1.41913 Å	1.43881 Å	1.45333 Å
12O-13H	0.96547 Å	0.97127 Å	0.96714 Å
∠9H-1C-10H	121.52019°	121.12530°	121.37374°
∠1C-6O-7O	107.67998°	105.64040°	106.34400°
∠6O-7O-8H	86.89771°	86.61178°	86.89728°
∠7O-8H-2O	146.69156°	147.12453°	148.55719°
∠4H-3C-5H	111.08053°	111.04908°	111.28227°
∠2O-3C-11O	105.79410°	104.53942°	105.03220°
∠11O-12O-13H	101.55860°	100.63096°	100.11481°

Product (HOOCH2OCH2OOH) of channel 3 $CH_2OO + HOCH_2OOH \rightarrow HOOCH_2OCH_2OOH$

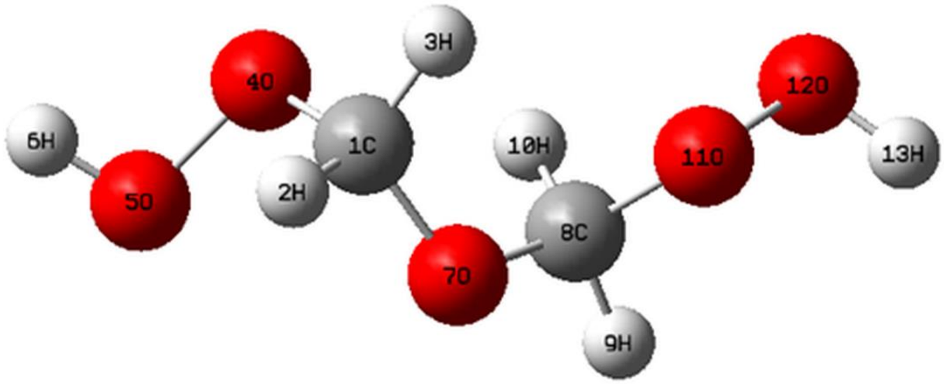

Geometrical parameters	M06-2X/AVTZ	MN15-L/AVTZ	B2PLYP-D3/AVTZ
1C-2H	1.08771Å	1.10255 Å	1.08612 Å
1C-3H	1.09170 Å	1.10746 Å	1.09074 Å
1C-4O	1.39672 Å	1.39722 Å	1.40154 Å
4O-5O	1.42583 Å	1.44972 Å	1.46090 Å
5O-6H	0.96458 Å	0.96980 Å	0.96652 Å
1C-7O	1.39939 Å	1.40716 Å	1.40780 Å
7O-8C	1.38287 Å	1.38878 Å	1.38911 Å
8C-9H	1.08980 Å	1.10588 Å	1.08848 Å
8C-10H	1.09174 Å	1.10793 Å	1.08971 Å
8C-11O	1.42554 Å	1.42702 Å	1.43456 Å
11O-12O	1.41929 Å	1.44029 Å	1.45334 Å
12O-13H	0.96459 Å	0.97001 Å	0.96634 Å
∠6H-5O-4O	100.78414°	99.67726°	99.23160°
∠5O-4O-1C	107.39314°	106.45920°	106.87260°
∠1C-7O-8C	114.12535°	113.25369°	114.21163°
∠8C-11O-12O	106.00988°	105.34535°	105.54262°
∠11O-12O-13H	101.71849°	100.76948°	100.28414°
∠2H-1C-3H	112.09763°	112.19387°	112.26838°
∠9H-8C-10H	111.08635°	110.82872°	111.29503°

Figure S5 Optimized geometries of the reactants, reactant complex, transition state, product complex and separate products of the $HOCH_2O(O)CH_2OOH + SO_2 \rightarrow HOCH_2OCH_2OOH + SO_3$ reaction at the M06-2X/AVDZ level using ultrafine grids

Reactants

$OHCH_2O(O)CH_2OOH$

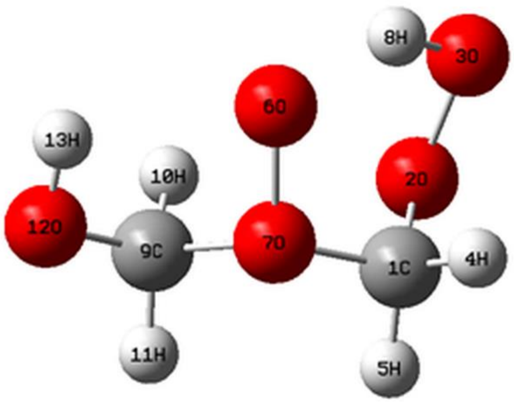

Cartesian coordinates of the optimized geometry

1.	C	-2.10452400	0.16023100	0.84983800
2.	O	-2.64371500	-0.19906600	-0.34916900
3.	O	-2.06311600	-1.43610400	-0.75796300
4.	H	-1.90263900	-0.69381000	1.50207500
5.	H	-2.74160600	0.93235800	1.29623500
6.	O	0.08842100	-0.14120800	-0.00125700
7.	O	-0.78734700	0.78754100	0.68138200
8.	H	-1.10355400	-1.17814700	-0.73376000
9.	C	-0.80567500	2.00556300	-0.17174800
10.	H	-1.21442200	1.66552800	-1.13042000
11.	H	-1.44480100	2.72580600	0.34975000
12.	O	0.46806700	2.47045300	-0.22309300
13.	H	1.00455900	1.73033700	-0.55542700

SO_2

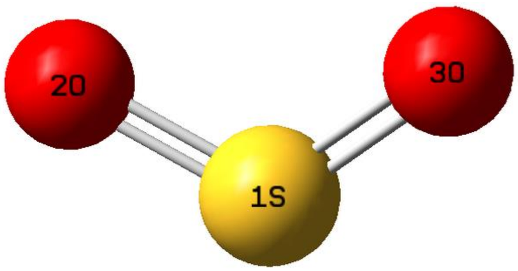

Cartesian coordinates of the optimized geometry

1.	S	1.88850900	-0.29859300	-0.33772500
2.	O	2.11281200	0.90461600	-1.14203700
3.	O	2.62773400	-0.41178300	0.92154200

Reactant complex of the $HOCH_2O(O)CH_2OOH + SO_2 \rightarrow HOCH_2OCH_2OOH + SO_3$ reaction

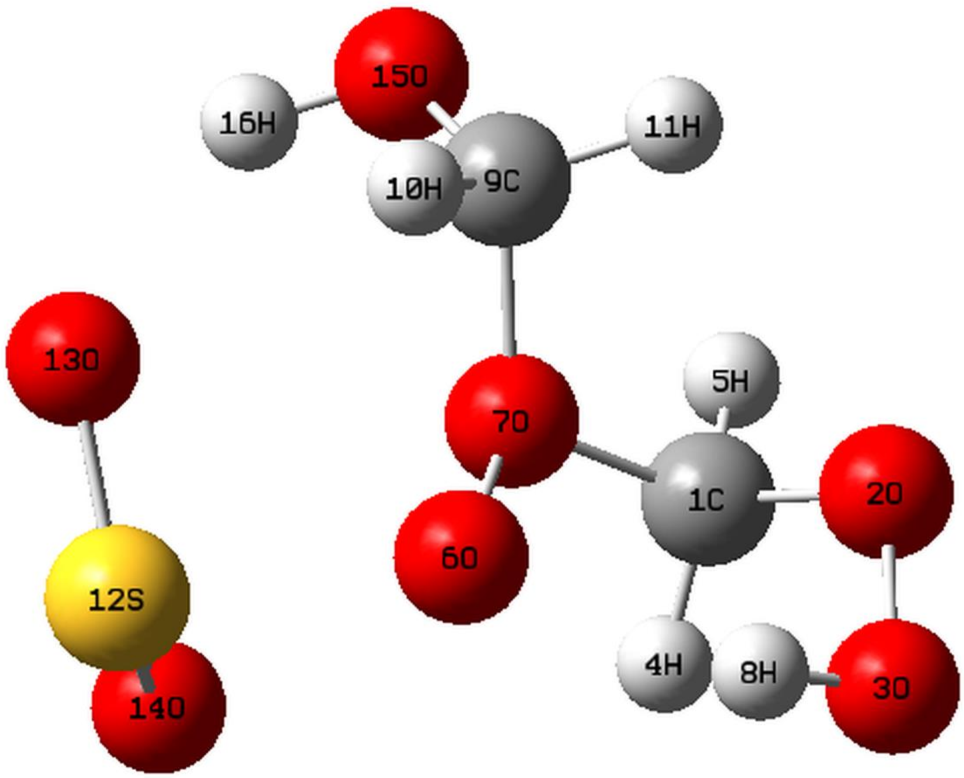

Cartesian coordinates of the optimized geometry

1.	C	-1.71199500	-0.13476600	1.03298000
2.	O	-2.82995200	-0.38889000	0.29348200
3.	O	-2.77219600	-1.72244800	-0.19655300
4.	H	-1.32767300	-1.01103000	1.56096400
5.	H	-1.90005800	0.73929200	1.66580200
6.	O	-0.24914400	-0.74886500	-0.74158700
7.	O	-0.60212100	0.28189900	0.16918000
8.	H	-1.99906500	-1.67843300	-0.79314500
9.	C	-0.72700200	1.62554100	-0.52393400
10.	H	-0.22410100	1.41584300	-1.46977300
11.	H	-1.79694900	1.82883500	-0.62033000
12.	S	1.88482800	-0.65817600	-0.25536100
13.	O	2.00196600	0.81255600	-0.47335500
14.	O	1.76043200	-1.02557500	1.16627600
15.	O	-0.13514600	2.53679300	0.27752300
16.	H	0.82036700	2.34240000	0.26535600

Transition state of the $HOCH_2O(O)CH_2OOH + SO_2 \rightarrow HOCH_2OCH_2OOH + SO_3$ reaction

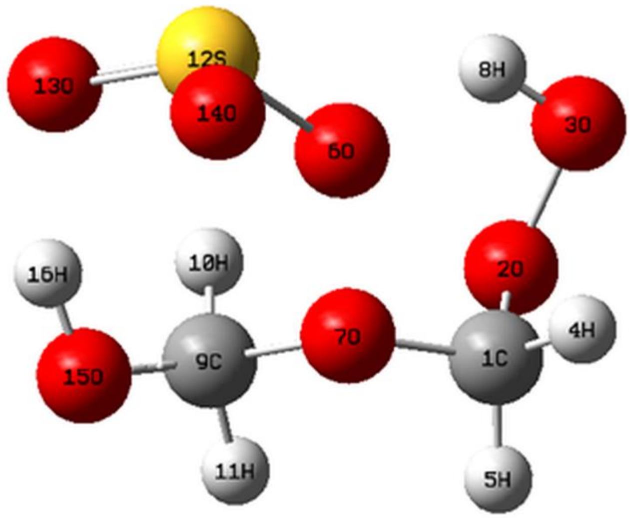

Cartesian coordinates of the optimized geometry

1.	C	-2.06125400	0.17878600	0.89248700
2.	O	-2.65259300	-0.16297800	-0.30196800
3.	O	-2.29903200	-1.49463600	-0.64052600
4.	H	-1.88766300	-0.68977200	1.53239900
5.	H	-2.68732100	0.94827800	1.36187700
6.	O	0.17500800	-0.35619800	-0.04113600
7.	O	-0.76367800	0.79226900	0.70888200
8.	H	-1.38688500	-1.39153400	-0.96358600
9.	C	-0.74349400	1.98668300	-0.20316100
10.	H	-0.90855600	1.57922800	-1.20652800
11.	H	-1.58426600	2.59225400	0.15625800
12.	S	1.87433900	-0.32189100	-0.33744900
13.	O	2.12137900	0.91910000	-1.14258700
14.	O	2.63333700	-0.40297000	0.92181600
15.	O	0.40978000	2.64933700	-0.02600200
16.	H	1.13960200	2.19776600	-0.51255300

Product complex of the $HOCH_2O(O)CH_2OOH + SO_2 \rightarrow HOCH_2OCH_2OOH + SO_3$ reaction

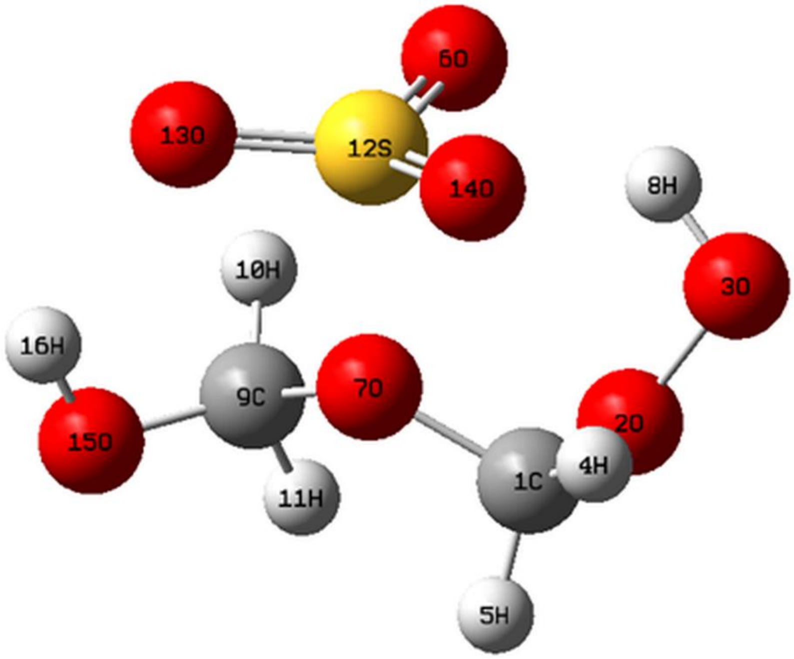

Cartesian coordinates of the optimized geometry

1.	C	-1.68535300	-0.08752100	1.08466700
2.	O	-2.48626200	-0.66145300	0.11966400
3.	O	-2.01065800	-1.97067900	-0.15332400
4.	H	-1.26640200	-0.83536000	1.76354900
5.	H	-2.29184200	0.67064700	1.59295900
6.	O	0.36525600	-1.01832700	-1.36694200
7.	O	-0.55349500	0.60592200	0.51935500
8.	H	-1.33507800	-1.81592200	-0.83954300
9.	C	-0.85025100	1.72256900	-0.38633600
10.	H	-0.61013300	1.36684800	-1.39566200
11.	H	-1.91758300	1.93928400	-0.28706100
12.	S	1.00533400	-0.46729000	-0.16622700
13.	O	1.87115000	0.69363400	-0.35590000
14.	O	1.15905000	-1.31821800	1.00089700
15.	O	-0.13504200	2.82188700	0.00109500
16.	H	0.80052900	2.66130500	-0.18766300

Separate products of the $HOCH_2O(O)CH_2OOH + SO_2 \rightarrow HOCH_2OCH_2OOH + SO_3$ reaction

$OHCH_2OCH_2OOH$

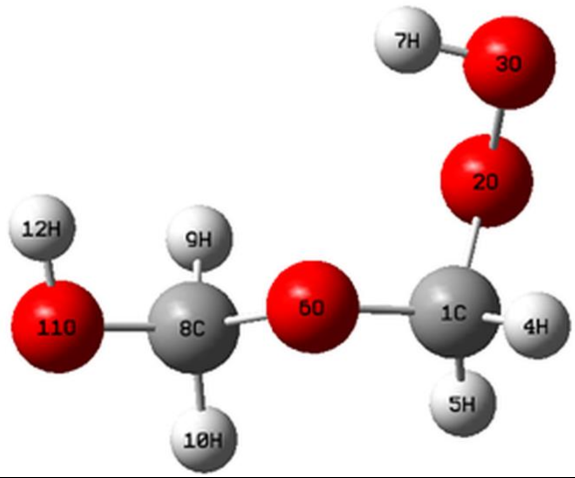

Cartesian coordinates of the optimized geometry

1.	C	-2.10332000	0.23145200	0.84122200
2.	O	-2.64142200	-0.31591300	-0.33682600
3.	O	-1.93352100	-1.51602400	-0.60298100
4.	H	-2.02560500	-0.54308100	1.61095000
5.	H	-2.82086200	1.01928300	1.11940700
6.	O	-0.81948000	0.74247600	0.64376300
7.	H	-1.08786300	-1.18757000	-0.94475200
8.	C	-0.81611700	1.97119400	-0.07450200
9.	H	-1.28441600	1.81546800	-1.05939300
10.	H	-1.37420400	2.72871100	0.49386000
11.	O	0.48774600	2.42751500	-0.17560900
12.	H	0.99370500	1.81217000	-0.71756000

SO_3

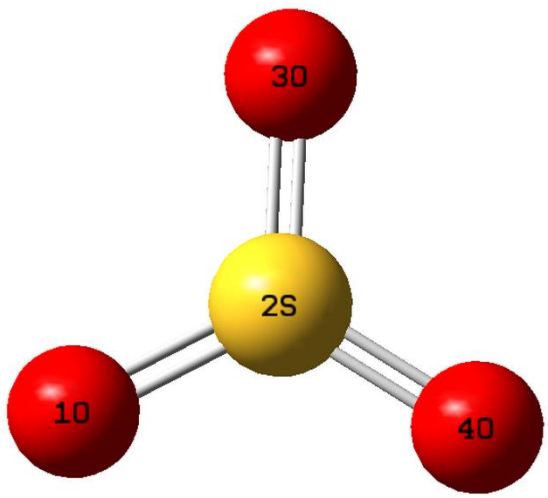

Cartesian coordinates of the optimized geometry

1.	O	0.30802800	-0.44926900	-0.08908600
2.	S	1.70111200	-0.04098500	-0.15027400
3.	O	2.15611300	0.83334900	-1.21768700
4.	O	2.63881000	-0.50505500	0.85769200

Figure S6 *VMEP*, ΔZPE and ΔV_a^G curves of channel 2 CH_2OO + $HOCH_2OOH \rightarrow HOCH_2O(O)CH_2OOH$ from POLYRATE calculations at the BD(T)/AVTZ//B2PLYP-D3/AVTZ level(energies in are kcal.mol^{-1} with respect to separate reactants).